

Effect of Substrate Crystalline Morphology on the Durability of PECVD Thin SiO_x Coatings

G. Rochat¹, Y. Leterrier¹, J.-A. E. Månson¹, R. Szoszkiewicz², A. J. Kulik², P. Fayet³

¹*Laboratoire de Technologie des Composites et Polymères (LTC),*

Ecole Polytechnique Fédérale de Lausanne (EPFL), CH-1015 Lausanne, Switzerland

²*Laboratoire de spectroscopie mécanique et nano-mécanique (LSMN), Institut de physique
de la matière complexe (IPMC),*

Ecole Polytechnique Fédérale de Lausanne (EPFL), CH-1015 Lausanne, Switzerland

³*Tetra Pak (Suisse) SA, Plasma Technology, C.P. 32, CH-1680 Romont, Switzerland*

Introduction

Thin oxide coatings such as those formed by plasma assisted processes on polymers find widespread use in numerous fields, including optoelectronics^[1,2] and pharmaceutical and food packaging^[3,4]. The functional performance of these layered composite systems depends on i) the cohesive strength of the brittle coating and ii) its adhesion to the polymer substrate. These two factors are controlled by the defect structure of the coating and of the interfacial region, and by the level of process-induced internal stresses^[5,6]. Whereas defects and internal stresses in thin oxide films have been extensively studied^[5-7], the influence of the substrate surface morphology has often been neglected in previous works, especially in case of semi-crystalline polymers. The present work analyzes effect of crystalline structures on the damage mechanisms of silicon-oxide coatings on semi-crystalline polymers, by means of uniaxial fragmentation tests and scanning local-acceleration microscopy.

Materials

Thin silicon oxide coatings (SiO_x) were deposited by plasma enhanced chemical vapor deposition (PECVD) from hexamethyldisiloxane vapor (HMDSO) on semi-crystalline 0.5 mm thick polyamide12 (PA12, Grilamid L25 EMS-Chemie) substrates. Two types of PA12 substrates were analyzed and the results are reported in Table 1. As-received substrates, characterized by the presence of large (radius~15 μm) crystalline spherulites, and substrates annealed at 220°C, above the melting point, and quenched, characterized by the absence of large crystalline structures. A crystallinity of 55% was measured for both substrates by differential scanning calorimetry (DSC). The coating thickness was 90 nm as measured by X-Ray fluorescence (XRF). The coating internal stresses have not been measured due to the large thickness of the substrate. The Young's moduli, E, of the two types of polymers and of their surface crystalline layers were measured by means of tensile tests and nanoindentation using a Berkovich indenter with R~150 nm, respectively. The defective amorphous zones of the as-received PA12, resulting from the impingement of the spherulites, were not

characterized by nanoindentation due to the artifacts induced by the size of the indenter. The RMS roughness of the samples was averaged on 20 $50 \times 50 \mu\text{m}^2$ AFM scans.

Table 1: Values of roughness, crystallinity and Young's modulus for the two materials.

Materials type	RMS Roughness [nm]	Crystallinity [%]	$E_{\text{tens.}}$ [GPa]	$E_{\text{nano.}}$ [GPa]
PA12 as-received	92 ± 5	55	1.54	1.40*
PA12 quenched	18 ± 3	55	1.67	1.35

(*) measured on spherulites

Scanning local-acceleration microscopy

Local mechanical properties of the substrates surface were investigated by means of scanning local-acceleration microscopy (SLAM), in order to determine qualitatively the stiffness contrast between the defective amorphous and crystalline zones of the as-received PA12. SLAM utilizes an atomic force microscope (AFM) cantilever to evaluate the surface elastic properties^[8]. A piezoelectric plate vibrates the sample far beyond the first resonance of the probing AFM cantilever. The interaction between the cantilever and the samples allows then to determine, at least qualitatively, the stiffness contrast between different regions of the sample surface. The determination of the maximum amplitude for each investigated zone allows the comparison of stiffness, knowing that a stiffer material will give rise to a higher frequency resonance. The results obtained for the as-received PA12 spherulitic and inter-spherulitic zones are shown in Fig. 1, which leads to the conclusion that the inter-spherulitic zones are softer than the spherulitic ones, due to their lower resonance frequency. In order to get quantitative evaluation of the Young's modulus, a tip-sample interaction model is required, which is yet to be developed in the case of soft polymer substrates. Nevertheless, the Young's moduli of the different phases have been determined by means of tensile tests and nanoindentation measurements (Table 1). These denote that, although the Young's modulus of the as-received PA12 is lower than the one of the quenched PA12, the latter has the same Young's modulus as the crystalline zones of the former. The presence of soft amorphous inter-spherulites zones leads to a decrease of the as-received PA12 stiffness compared to the homogeneous quenched PA12.

Uniaxial fragmentation

Uniaxial fragmentation tests^[9] were carried out in-situ in an optical microscope (Olympus BHS2) on both films to determine the SiO_x cohesive strength and the $\text{SiO}_x/\text{PA12}$ interfacial shear strength. The samples were loaded stepwise up to predefined nominal strain levels, ϵ . The crack density, defined as the inverse of the average fragment length, was determined, at each selected strain, by dividing the number of cracks counted on a micrograph by the

micrograph length, and multiplying the result by $(1+\epsilon)$ in order to take into account, to a first approximation, the crack opening.

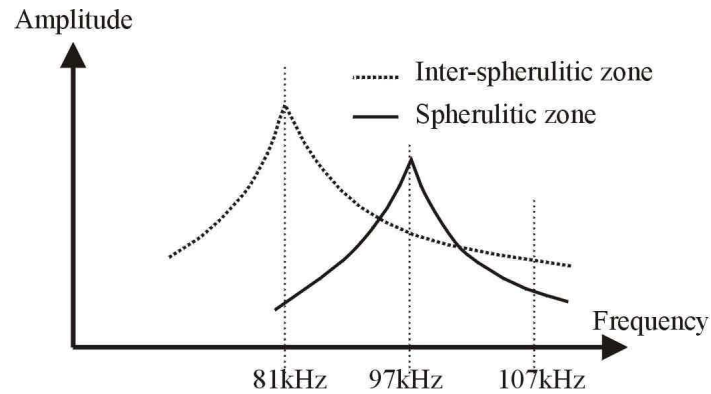


Figure 1: Amplitude response of the SLAM of the two PA12 substrates.

Fragmentation of SiO_x /as-received PA12 samples revealed preferential delamination of the coating at the spherulites boundaries, in the form of coating buckles due to substrate Poisson contraction (Fig. 2a)^[10]. For the quenched PA12 substrate (Fig. 2b), such underlying structures are not present, and the buckling phenomena appear in this case to be correlated with microscratches of the quenched PA12 surface. Damage in the coating is thus driven by superficial heterogeneities of the polymer spherulites boundaries in the as-received PA12, and of surface microscratches and defects in the quenched PA12.

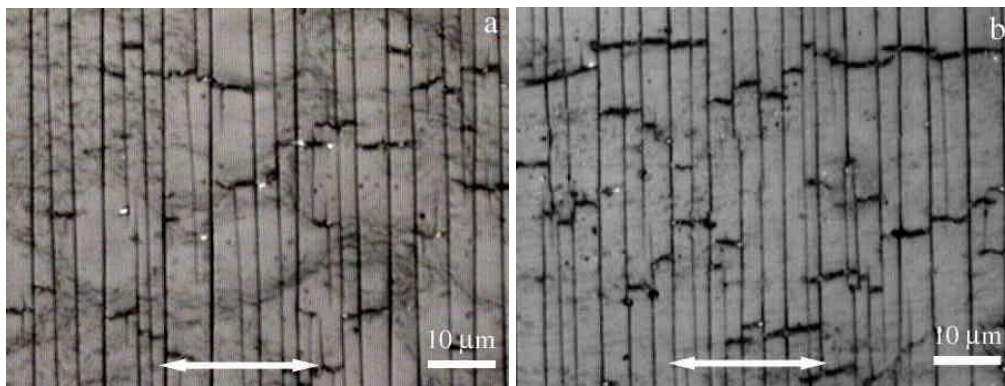


Figure 2: Fragmentation pattern for SiO_x coatings on as-received PA12 (a), and quenched PA12 (b) at 4.5% strain. The arrows indicate the loading direction.

The overall evolution of damage in the oxide upon tensile loading is shown in Fig. 3 for the two types of PA12 substrates. The coating crack onset strain (COS) of the SiO_x coating was measured to be equal to 1.2% in the case of the as-received PA12 substrate, and to 1.4% with the quenched PA12 substrate. In the former case, the lower COS is attributed to a higher defect density. Ongoing work is devoted to examine this hypothesis, and determine accurately the cohesive strength of the oxide. The density of cracks at saturation in the coating is higher in the case of the quenched substrate, which, for an equivalent cohesive strength, would imply a better adhesion. The determination of the oxide strength will enable

the calculation of the interfacial shear strength between the oxide and each of the two types of PA12 substrates^[11].

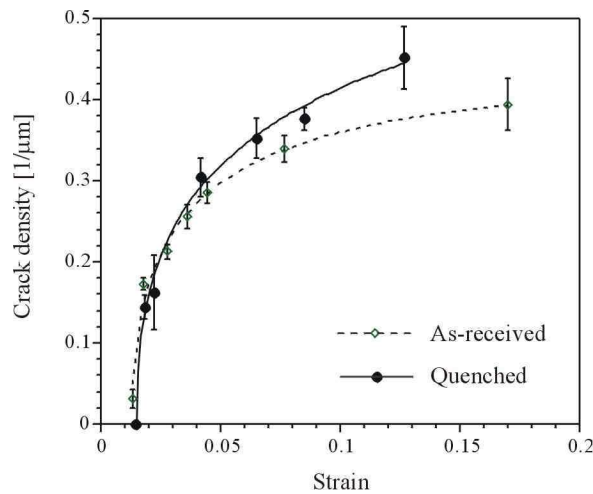


Figure 3: Crack density vs. strain curves for the SiO_x coating on as-received and quenched PA12.

Conclusions

Superficial surface heterogeneities of semi-crystalline polymers, such as amorphous defective regions, or microscratches, are determinant for the damage of thin PECVD oxide films. In case of spherulitic structures, it was shown by means of SLAM measurements that the crystalline zones are stiffer than the amorphous ones, which promotes strain concentrations at the spherulites boundaries. Moreover, fragmentation tests suggest that the adhesion of the coating is better on quenched PA12 with homogeneous and smooth surface structure, than on the as-received PA12 which presents large crystalline structures, with 5-fold roughness increase.

Acknowledgements

G.R. and Y.L. acknowledge Tetra Pak (Suisse) SA, Plasma Technology for financial support.

References

1. SARTO, F. et al. *Thin Solid Films* **346**, 196-201 (1999).
2. AFFINITO, J. D. et al. *Thin Solid Films* **290-1**, 63-7 (1996).
3. CHATHAM, H. *Surf. Coat. Technol.* **78**, 1-9 (1996).
4. WALTHER, M., HEMING, M. & SPALLEK, M. *Surf. Coat. Technol.* **80**, 200-2 (1996).
5. ROCHAT, G. et al. *Proc. Journées d'études sur l'adhésion JADH'01* 46-9 (Cap-Ferret, 2001).
6. LETERRIER, Y., WYSER, Y. & MÅNSON, J.-A. E. *J. Adh. Sci. Technol.* **15**, 841-65 (2001).
7. SOBRINHO, A. S. D. S. et al. *Proc. 42nd SVC Ann. Conf.* 1-5 (Chicago, 1999).
8. BURNHAM, N. A. et al. *J. Vac. Sci. Technol. B* **14**, 794-9 (1996).
9. LETERRIER, Y. et al. *J. Polym. Sci. B: Polym. Phys.* **35**, 1463-72 (1997).
10. ROCHAT, G. et al. *Proc. ECASIA'2001, Avignon (F)* (2001).
11. LETERRIER, Y. et al. *J. Polym. Sci. B: Polym. Phys.* **35**, 1449-61 (1997).